A Biophysical Investigation on the Binding and Controlled DNA Release in a Cetyltrimethylammonium Bromide−Sodium Octyl Sulfate Cat-Anionic Vesicle System

Adalberto Bonincontro,[†,‡] Camillo La Mesa,[‡,§] Carla Proietti,[†,||] and Gianfranco Risuleo*[,†,‡,⊥]

CNISM-Dipartimento di Fisica, SOFT-INFM-CNR Research Centre, Dipartimento di Chimica, and Dipartimento di Genetica e Biologia Molecolare, Università di Roma "La Sapienza", P. le A. Moro 2, I-00185 Roma, Italy

Received December 21, 2006; Revised Manuscript Received March 29, 2007

The interactions between cat-anionic (an acronym indicating surfactant aggregates (micelles and vesicles) formed upon mixing cationic and anionic surfactants in nonstoichiometric amounts) vesicles and DNA have been the subject of intensive studies because of their potential applications in biomedicine. Here we report on the interactions between DNA and cetyltrimethylammonium bromide (CTAB)−sodium octyl sulfate (SOS) cat-anionic vesicles. The study was performed by combining dielectric relaxation spectroscopy, circular dichroism, dynamic light scattering, ion conductivity, and molecular biology techniques. DNA is added to positively charged vesicles until complete charge neutralization of the complex and formation of lipoplexes. This occurs when the mole ratio between the phosphate groups of DNA and positive charges on the vesicle is about 1.8. Above this threshold the nucleic acid in excess remains free in solution. This very interesting new result shows that anionic surfactants are not expelled upon saturation, and therefore, no formation of micelles occurs. Furthermore, vesicle-bound DNA can be released in its native form, as confirmed by dielectric spectroscopy and circular dichroism measurements. The nucleic acid is released upon addition of SOS, which competes with the phosphate groups of the DNA: this results in the demolition of the CTAB−SOS cat-anionic vesicles. These results indicate the possibility of a controlled DNA release and might be of interest in biomedicine.

Introduction

The interactions between cat-anionic systems and biopolymers, in particular DNA, raised a growing interest during recent years. Cat-anionic is an acronym indicating surfactant aggregates (micelles and vesicles) formed upon mixing cationic and anionic surfactants in nonstoichiometric amounts. The interactions of such aggregates with biopolymers involve complicated methodological aspects, which have interesting thermodynamic, structural, biomedical, and biophysical implications.[1−4] The formation of DNA/cat-anionic complexes can become useful for DNA delivery into cells, through membrane fusion and/or endocytosis. These complexes, also termed "lipoplexes", constitute a valid system for DNA delivery into the cell nucleus.[5−7] Furthermore, these vesicles are easily prepared and assemble spontaneously, simply mixing, in proper mole ratios, cationic and anionic surfactants. The resulting vesicles are stable and have a long shelf life, and their cytotoxicity is low.[8] Their low cost makes them advantageous with respect to liposomes made by natural or synthetic lipids.[9−12]

From a theoretical point of view, the interactions between DNA and cat-anionic vesicles are mainly due to electrostatic bonds of the macromolecule with the excess positive charges exposed to the surfactant aggregates, but an increase of the counterion entropy plays a possible role.[5,6,13] Cat-anionic vesicles adsorb the polyion, up to the charge neutralization threshold, presumably reaching a putative point of zero charge. However, an exhaustive description of the aggregation process is yet to be elucidated. For instance, the mode of preparation may influence the final structure of the vesicles[14] and of DNA/vesicle complexes.[6]

Previous studies demonstrate that, above the point of zero charge, DNA/vesicle complexes coexist with the free nucleic acid in solution.[15,16] Some authors, conversely, postulate that when the DNA concentration increases, a structural rearrangement is triggered, consisting in the formation of double amphiphile layers where the nucleic acid is packaged.[17]

Cryogenic transmission electron microscopy (cryo-TEM), fluorescence methods, and small-angle X-ray scattering (SAXS) traditionally were used to study these systems.[18−21] To investigate the formation of DNA/vesicle complexes, we chose an approach based on the combined use of biophysical and biomolecular techniques, such as dielectric relaxation spectroscopy (DS), circular dichroism (CD), ionic conductivity, dynamic light scattering (DLS), and agarose gel electrophoresis (AGE). The combination of different experimental methods has some advantages with respect to more sophisticated approaches based on SAXS or cryo-TEM. In particular, the present techniques allow following directly the dynamics of formation of the DNA/vesicle complexes. Furthermore, the molecular conformation of the biopolymer during the binding process can be monitored.

Materials and Methods

Surfactants. The CTAB−SOS cat-anionic system used in this work is an aqueous mixture made of cetyltrimethylammonium bromide

* Author to whom correspondence should be addressed. E-mail: gianfranco.risuleo@uniroma1.it.

† CNISM-Dipartimento di Fisica.

‡ SOFT-INFM-CNR Research Centre.

§ Dipartimento di Chimica.

|| Present address: Dipartimento di Medicina Sperimentale e Scienze Biochimiche, Università di Perugia, Perugia, Italy.

⊥ Dipartimento di Genetica e Biologia Molecolare.

10.1021/bm0612079 CCC: $37.00
Published on Web 05/15/2007

(CTAB) and sodium octyl sulfate (SOS). Surfactants were obtained from Sigma-Aldrich. The surfactants are commercially available at high purity (over 99.0%) and were used without further purification. The vesicles were prepared by mixing two different solutions of CTAB and SOS to get a total surfactant concentration of 21.6 mM (11.85 mM CTAB and 9.75 mM SOS). The excess positive charges in the resulting vesicle are 2.1 mM. The ternary phase diagram for the system CTAB−SOS−H_2O is reported in the literature.[22] Attention was focused on getting samples in the narrow concentration regime pertinent to the existence of vesicles. No salts or buffers were used, to modulate the electrostatic interactions between vesicles and DNA and to minimize the screening of such interactions.

DNA. Calf thymus DNA sodium salt (ctDNA-Na) was from Sigma-Aldrich. It was dissolved in deionized water and fragmented by ultrasonic waves with a VCX 600 Vibra Cell sonicator, Sonics and Materials Inc. The working conditions were 5 mg/mL concentration and 1 min sonication time, at 20 kHz and 600 W.[23] After fragmentation, agarose gel electrophoresis and densitometric scanning estimated the average DNA distribution. The size of the main population fragments resulting from the sonication procedure spanned 500−1000 base pairs (bp's).

The concentration of nucleic acid was increased from 0 to 15 mM (expressed in terms of phosphate groups), while the surfactant concentration in the vesicle mixture was kept constant to 21.6 mM (11.85 mM CTAB and 9.75 mM SOS).

Methods. *Dielectric Spectroscopy.* The measuring apparatus consists of a computer-controlled HP impedance analyzer, model 4194A, working in the 0.1−100 MHz range. The measuring cell, previously described,[24] is a section of a cylindrical waveguide and can be partially filled with the sample. The system behaves as a waveguide excited far beyond its cutoff frequency mode. Therefore, only the stray field in the transition from the coaxial line to the waveguide is used. Cell constants were determined by an interpolation method based on measurements with electrolyte solutions of known conductivity, close to those of the samples under test, following a standard procedure.[25,26] The errors were within 1% on both the real, ϵ', and the imaginary, ϵ'', parts of the complex dielectric constant ϵ^*. The dielectric relaxation loss was obtained after subtraction of the ionic contribution $\sigma/\epsilon_0\omega$, where σ is the sample conductivity, ω the angular frequency of the applied electric field, and ϵ_0 the vacuum dielectric constant. The measuring cell was thermally controlled to 20.0 ± 0.1 °C.

Ion Conductivity. Conductance measurements were carried out with an accuracy of ±0.05% using a Wayne-Kerr model 6425 precision component analyzer. The electrical resistance of the solutions, measured at 1.0, 2.0, 5.0, and 10 kHz, was extrapolated to infinite frequency for the usual corrections. The measuring cell is located in an oil bath, at 20.000 ± 0.003 °C. Measurements were performed by adding known amounts of DNA in the CTAB−SOS pseudosolvent to the bare vesicular system by a weight buret, under stirring, and recorded 10 min after each addition.

Laser Light Scattering. A Brookhaven digital correlator (BI 9000AT), equipped with a 632.8 nm 10 mW He−Ne laser source, performed DLS experiments at 90°. The samples were located in cuvettes at 20.00 ± 0.05 °C. The detector consists of a photomultiplier and an amplifier, working as pulse selectors. Details on the apparatus and on the measuring procedures can be found elsewhere.[27] The relaxation times (1/Γ) were determined by a CONTIN program, working in terms of a continuous distribution of exponential decay times.[28] Errors in the average particle size were ±5%. The corresponding size-distribution functions are monodisperse.

DLS measurements were performed at fixed surfactant content and CTAB/SOS ratio while the DNA concentration was increase. This can be done by adding lyophilized DNA to the vesicular pseudosolvent and stirring the resulting mixtures until equilibrium is obtained or adding known amounts of concentrated DNA−CTAB/SOS suspensions to the vesicles upon stirring. The values of $\langle R_H \rangle$ resulting from the two sets of data are equivalent, provided the equilibration time between preparation and measurement is adequately long (about 20 min).

Circular Dichroism. The samples are located in 1.00 cm path length cuvettes, and CD spectra were collected using a Jasco J-810 spectropolarimeter equipped with a Peltier temperature control device, at 20.0 ± 0.1 °C. The spectral resolution is ±0.1 nm. The UV CD spectrum of calf thymus DNA exhibits a positive band at 275 nm, due to the base stacking, and a negative peak at 245 nm, ascribed to the DNA double helix structure. As a rule, modification in the maximum peak wavelength is moderate, if any.

Agarose Gel Electrophoresis. Typical operating conditions were 1.5% agarose (w/v) and 5 V/cm at room temperature in TEA buffer, pH 7.5 (Tris−HCl and EDTA, 50 and 5 mM, respectively). DNA was visualized by ethidium bromide (0.5 μg/mL fc), and a standard DNA ladder of 100 bp multimers was used as a reference.

In experiments requiring centrifugation, the samples were run at room temperature for 5 min at 2000*g*.

Results and Discussion

Vesicle Properties. Vesicles formed by mixtures of oppositely charged surfactants are stable as compared to lipid-based ones.[14,29] Even prolonged centrifugation does not give rise to significant precipitation. The reasons for such unexpected behavior have been rationalized by Kaler,[30] who demonstrated that the vesicles have spontaneous bending and high thermodynamic stability when the ratio (κ/k_BT) is $\gg 1$ (κ is the energy curvature modulus). These are conditions quite different from those currently observed in lipid-based vesicles or the predictions by Helfrich, who supposed that the vesicle stabilization process is driven essentially by thermal fluctuations.[31] Kaler used former theories on the spontaneous curvature of vesicles[30b,c] and demonstrated that in mixtures of oppositely charged surfactants the following equality holds:

$$f_c = 2K\left(\frac{1}{R_1} - \frac{1}{R^\circ}\right)^2 \tag{1}$$

where f_c is the bending energy per unit area, R_1 the vesicle radius, and R° the spontaneous curvature of the bilayer and K ($2K = 2\kappa + \kappa^\circ$) indicates the balance between the κ modulus and the saddle-splay term, κ°. Proper handling of the above equation gives the size-distribution function of the vesicles, based on Boltzmann statistics, and ensures getting reasonable estimates of the most stable size. This can be done by analyzing the unimodal size distribution of vesicles obtained by DLS, and accordingly

$$\mu_N^\circ - \mu_M^\circ = \left(\frac{4\pi R_1^2}{N}\right)\left(2K\left(\frac{1}{R_1} - \frac{1}{R^\circ}\right)^2\right) \tag{2}$$

where μ_N° and μ_M° are the chemical potentials for the vesicles characterized by an R_1 radius. The subscript N (or M for the proper vesicle size) indicates the number of molecule in the vesicles, which is obtained by the equality

$$M = \frac{8\pi(R^\circ)^2}{A^\circ} \tag{3}$$

where A° is the average area per surfactant (in the mixture) at the air−aqueous solution interfaces.[32] Hence, the concentration for any given vesicle size is obtained by combining, for instance, results from DLS in terms of the above relations. The resulting agreement with the original theory is satisfactory. According to DLS, the average vesicle radius is close to 200 nm. The corresponding distribution function, evaluated by light scattering, is relatively narrow[33] and consistent with Kaler's hypothesis.[30]

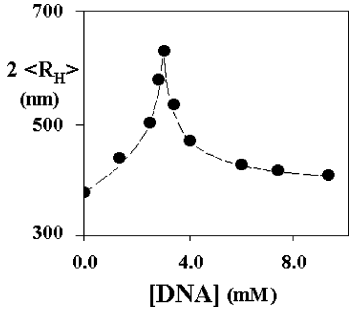

Figure 1. Average hydrodynamic diameter of the lipoplexes, $2\langle R_H \rangle$, in nanometers, as a function of DNA added to the vesicular dispersions at 20.0 °C. The nucleic acid content is expressed in terms of the phosphate molarity. The dotted line is for visual purposes.

Equations 1−3 do not explicitly account for the distribution of the surfactants between the inner and outer vesicle surfaces. It is commonly accepted, however, that the surfactants are distributed in regions of different curvature according to the requirements dictated by the packing constraint theory.[34] In mixtures, surfactants will be preferentially located in regions of lower curvature and vice versa, depending on their packing constraint ($H = V/A°L$). Here V is the volume of the hydrocarbon chain, $A°$ the area per molecule at the interface, and L the length of the alkyl chain in extended conformation. Taking into account the curvature radius of the CTAB and SOS micelles, it is reasonable that the latter molecules are preferentially located inside the vesicle and the CTAB ones line the outer surface. Estimates based on the packing constraint for a given vesicle size indicate that such an excess is 5−10% lower than supposed. The excess surface charge density (proportional to the CTAB content in the outer layer and modulated by partial replacement of CTA^+ with OS^- ions) will be reduced by a slightly higher amount. The nominal surface excess concentration reported above (2.1 mM) is an upper limit for the excess CTAB concentration in the outer vesicle layer.

DLS Measurements. The average particle size regularly increases as the amount of DNA in the medium is increased. The values of $\langle R_H \rangle$ reach a maximum at concentrations close to the charge ratio 1.8 (DNA^-/CTA^+), Figure 1. This is a consequence of lipoplex formation. Above the saturation point, the values of the hydrodynamic radius level off at higher macromolecule content, progressively approaching the $\langle R_H \rangle$ values pertinent to free DNA. It must be pointed out, however, that some precipitates occur at, or close to, the charge ratio mentioned above. Hence, the behavior in Figure 1 also indicates the depletion of some amounts of lipoplexes from the dispersions.

DS Measurements. This technique allows the formation of DNA/vesicle complexes to be followed. The measurements, at different DNA/vesicle ratios, were performed in the radio frequency range where all microheterogeneous systems (such as micelles, polyelectrolytes, and aqueous dispersions of vesicles) exhibit characteristic dielectric relaxation processes. Experiments were carried out at fixed vesicle concentration and increasing DNA content. The behavior of some mixtures, Figure 2, evidences modifications of the dielectric dispersion spectra, due to the interactions between vesicles and the nucleic acid.

Dielectric relaxation data were elaborated according to the classical Cole−Cole equation

$$\epsilon^* = \epsilon_\infty + \frac{\Delta\epsilon}{1 + (jf/f^*)^{1-\alpha}} \qquad (4)$$

where $j = \sqrt{-1}$ and $\Delta\epsilon$ is $\epsilon' - \epsilon_\infty$, f the measuring frequency, f^* the relaxation one, and α an empirical parameter taking into account the spreading of the relaxation times.

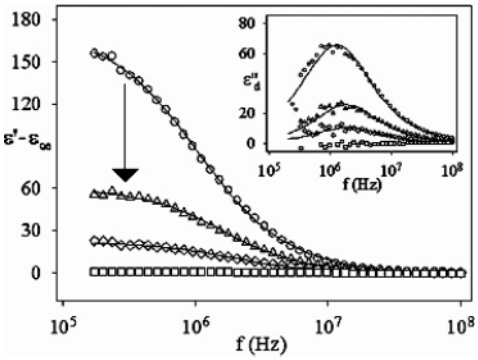

Figure 2. Dielectric dispersion of CTAB−SOS vesicle suspensions with increasing DNA content at 20.0 °C. Data are reported as $\epsilon' - \epsilon_\infty$ vs f, in hertz. The biopolymer concentration is expressed in terms of the phosphate molarity. The symbols refer to bare vesicles (○) and 1.5 (△), 2.5 (◇), and 3.5 (□) mM DNA. In the inset is drawn the behavior of the imaginary component ϵ_d'' vs log f, in hertz, for the same mixtures. The arrow indicates the progressive addition of DNA.

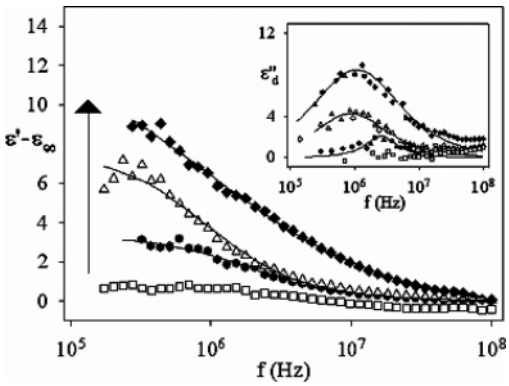

Figure 3. Dielectric dispersion of CTAB−SOS vesicles plus DNA at various concentrations, above binding saturation, at 20.0 °C. The nucleic acid concentration is 3.5 (□), 4.3 (●), 6.2 (△), and 9.3 (◆) mM, respectively. In the inset is drawn the behavior of the imaginary component ϵ_d'' vs log f, in hertz, for the same mixtures. The arrow indicates the progressive addition of DNA.

In the absence of DNA, a Maxwell−Wagner dielectric relaxation process, deriving from interfacial polarization, occurs.[35] The analysis of vesicle dispersions shows a significant dielectric increment ($\Delta\epsilon = 170 \pm 8$) and a relaxation frequency (f^*) occurring at 1.1 ± 0.1 MHz. The dispersion due to surface counterion conductivity in the double layer surrounding the vesicle is found in the kilohertz field for large particles such as these.[36] The interactions between the biopolymer and the vesicle neutralize the positive inner surface charges and dramatically reduce the dielectric increment down to a near zero value observed at 3.5 mM DNA. Further additions of the biopolymer cause an increase of the $\Delta\epsilon$ values, as can be inferred by the dispersion curves, Figure 3. The difference in dielectric increments is significant, whereas the information from the corresponding relaxation frequencies is not as reliable due to a much larger uncertainty. Above the saturation threshold, however, both $\Delta\epsilon$ and f^* are very close to the values observed in DNA solutions at comparable concentrations.[37]

In saturation conditions, the ratio $R = DNA^-/CTA^+$ is 1.8 (CTA^+ is the excess positive charge on the vesicles, and DNA^- is expressed in terms of the molarity of the phosphate groups). R represents binding saturation and is consistent with estimates of the vesicle charge.[38] The reasons why DNA does not interact stoichiometrically with vesicle charges are many-fold. In

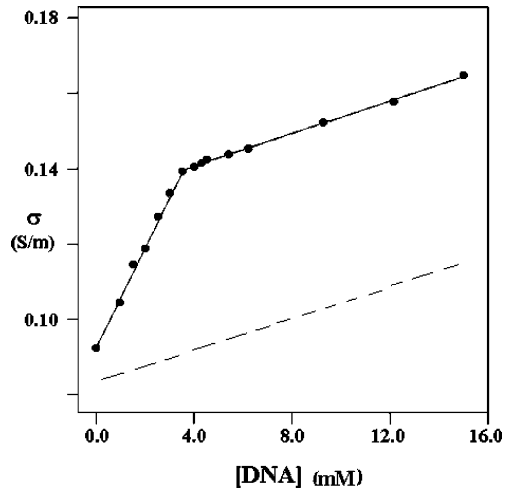

Figure 4. Ionic conductivity of vesicular dispersions (11.85 mM CTAB and 9.75 mM SOS), σ (S m^{-1}), as a function of the concentration (mM) of added DNA at 20.0 °C. For comparison, the behavior relative to that of bare DNA is reported as a dotted line.

particular, the geometry of charge distribution onto vesicles may not match completely that along the sugar−phosphate backbone.

Estimates of the average distance between positive charges on the vesicle were made assuming that the area of the CTAB polar head is 0.5−0.6 nm^2. Simple calculations show that the surface charge density is in the range $(3-4) \times 10^{-1}$ q nm^{-2}. This implies a distance between adjacent positive charges in the 2 nm range. Therefore, not all negative groups on the DNA backbone, located at a distance of 0.17 nm from one another, may interact with trimethylammonium groups, and charge neutralization may be not complete.

Cryo-TEM and SAXS show that DNA forms surface complexes and condenses within the vesicles where it may become incorporated into their bilayer. Accordingly, not all phosphate residues of DNA neutralize the positive surface charges on the vesicle. DNA compaction, thus, is an alternative interpretation. In this regard, Miguel suggested that DNA continues to be incorporated even after completion of saturation and causes the expulsion of anionic surfactants from the lipoplexes, thus giving rise to micelles.[5] This statement, however, is invalidated by our dielectric results, which indicate the presence of free DNA rather than micelles. As a matter of fact, the dielectric relaxation of these micelles occurs in an interval ranging from 10 to 50 MHz.[39,40] The relaxation observed beyond saturation occurs in the megahertz range, and this is indicative of the presence of free DNA fragments.[41]

Conductivity measurements also show the establishment of binding between DNA and vesicles, Figure 4. The ion conductivity increases, and a two-state linear trend is evident. It must be pointed out that the change of slope occurs at a DNA concentration of 3.8 mM, which implies $R = 1.8$. The first conductometric regime may be associated with the progressive DNA binding to vesicles; the second one reflects, on the other hand, the behavior after saturation. In fact, in the first region a release of Na^+ (from DNA) and Br^- (from the vesicles) is a consequence of the electrostatic interactions between the negative charges on the macromolecule and the positive charges facing outward from the vesicles. The second linear regime takes into account the increase of bulk Na^+ ions due to free DNA. Other ion mobility contributions can be neglected.

In a series of experiments we examined the possibility of a controlled release of DNA from the lipoplexes. To this aim an amount of SOS equivalent to the CTAB excess in the vesicles

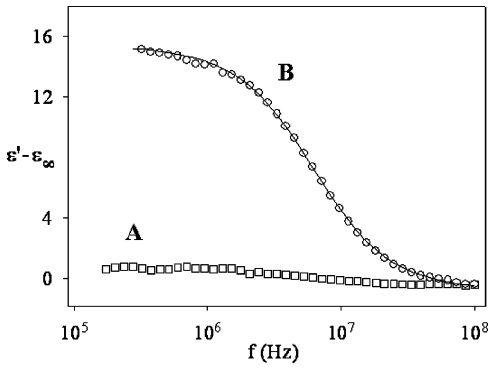

Figure 5. Dielectric response of the vesicle/DNA complex ($R = 1.8$) before (□) and after (○) addition of the surfactant in defect ([SOS] = 2.1 mM) at 20.0 °C.

was added. The addition was done in a condition of DNA/vesicle saturation ($R = 1.8$), where the dielectric response is near zero. The appearance of a significant dielectric relaxation is ascribable to free DNA (Figure 5). As a matter of fact, the dielectric parameters, obtained from a Cole−Cole fit of experimental data ($\Delta\epsilon = 16 \pm 0.8$, $\nu_r = 6.1 \pm 0.6$ MHz), strongly resemble those pertinent to free DNA in solution.[42]

Visualization of Free and Bound DNA by Gel Electrophoresis. AGE was used to visualize DNA−vesicle interactions. While vesicles alone cannot be separated from the solvent by centrifugation, on the contrary vesicle/DNA complexes do sediment upon centrifugation. Therefore, the complexes were centrifuged, and both the pellets (lanes P) and supernatants (lanes S) were run on AGE in the presence of ethidium bromide (EB) as the intercalating drug. The data in Figure 6 (upper panel) show that the fluorescence signal due to EB intercalated within the DNA double helix is visible in the supernatant only when the mole ratio R is higher than 1.8 (lanes S_6 and S_9). Obviously, at 0 mM DNA (lanes P_0 and S_0) no signal is evident. The pellets containing the complexes and resuspended in water show a negligible fluorescent signal, since bound DNA is substantially not accessible to the fluorophore. The very faint fluorescent signals observed in the presence of sedimented vesicle/DNA complexes is most likely due to the interaction of EB with some DNA tails extruding from the complex and/or adsorbed around it (lanes P_2-P_9).

The release of DNA was also examined. The complex obtained at binding saturation was divided into two aliquots. The first aliquot was centrifuged, the pellets were resuspended in water, SOS was added to reach the vesicle neutralizing concentration, and the liquid phase was run on AGE (lanes LA_0-LA_9). The second was directly supplemented with SOS, and run as above (lanes LB_0-LB_9). Results of these AGE runs (Figure 6, lower panel) show that vesicle-bound DNA can be completely released after addition of an adequate amount of SOS, and this also suggests that surfactant binding to CTAB is stronger than DNA−CTAB interactions in the vesicle. Thus, the nucleic acid can be efficiently forced out. These data are in substantial agreement with dielectric relaxation results.

CD Measurements. To investigate possible alterations of DNA structure, consequent to its interaction with vesicles, CD measurements were performed in the range 220−320 nm. In this region the spectrum of DNA in water shows a negative band at 249 nm and a positive one at 275 nm with a nodal point at about 258 nm. The spectrum refers to DNA in the classical B conformation.[43] The spectra of DNA/vesicle complexes at various mole ratios are shown in Figure 7. An overall resemblance is evident from a comparison of the two patterns,

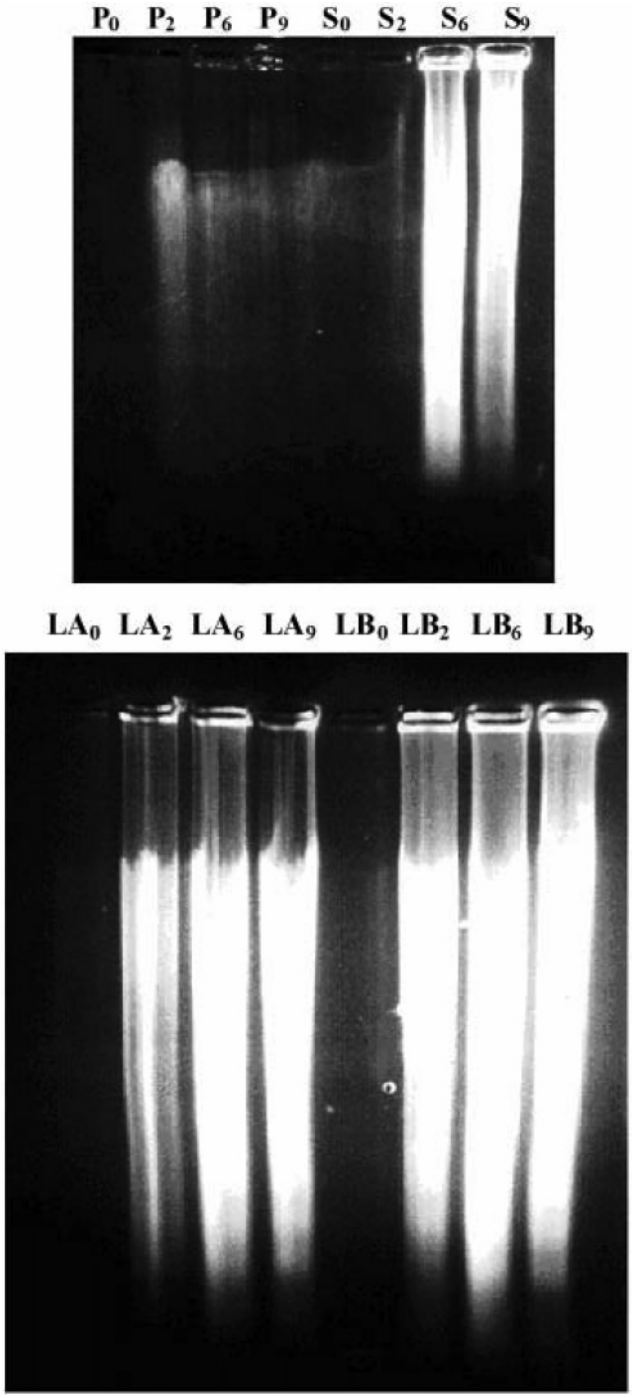

Figure 6. Pictures of electrophoresis runs showing the fluorescence of DNA-bound ethidium bromide. In the upper panel is reported the fluorescence due to increasing DNA in the vesicle (0−9 mM from the left to the right) for both the pellet (P) and supernatant (S). In the lower panel is reported the fluorescence monitored in the liquid phase obtained after addition of SOS.

although small variations in the band amplitudes are observed. The decrease in peak intensity is likely due to aggregation phenomena, causing a partial precipitation of the complexes, with a slight decrease of the actual DNA in solution. Therefore, it can be assumed that the vesicle-bound DNA substantially maintains its native conformation.

Conclusions

The purpose of this paper was to elucidate some aspects inherent to the adsorption and possible condensation of DNA onto synthetic vesicles. Results presented here show that the interaction is significant, with subsequent formation of lipoplexes, which precipitate out. Unexpectedly, the formation of lipoplexes is not stoichiometric in terms of nominal charges. It is possible, in addition, to recover the biomacromolecule by adding anionic surfactants in such amounts to fully neutralize the vesicle charge and precipitating CTAB as a nonsoluble salt. In some aspects, use of vesicular systems reduces the undesired precipitation effects observed when DNA, or its gels, is mixed with quaternary ammonium salts only.[44,45]

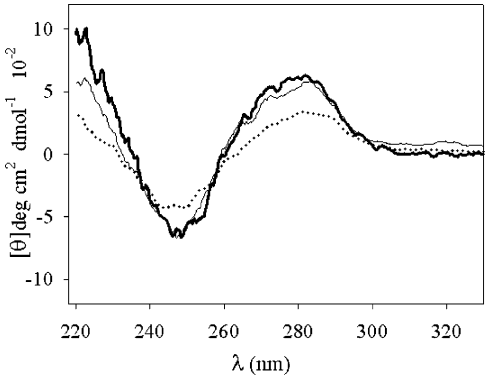

Figure 7. Circular dichroism spectra of DNA bound to CTAB−SOS vesicles at 20.0 °C: thick line, 0.96 mM DNA; thin line, 1.94 mM DNA; dotted line, 2.26 mM DNA. The total surfactant concentration is 21.6 mM, and the CTAB excess is 2.1 mM.

The reasons underlying this complex phenomenology are many-fold and are presumably due to a combination of binding and compaction onto polydisperse vesicles. According to recent studies, it is stated that the size and polydispersity index of the vesicles are relevant in the completion of the binding processes.[16] The entry of DNA into vesicles and the subsequent release from the anionic surfactants[5,6] are not realistic, at least in the present experimental conditions.

Some aspects peculiar to DNA binding onto the vesicles, perhaps, require the use of more performance-oriented instrumental facilities, giving the possibility to investigate the electrophoretic mobility of the macromolecule, the vesicles, the resulting lipoplexes, and the corresponding charge density. It is expected that the latter results are complementary to those obtained by dielectric relaxation spectroscopy, which indicate the occurrence of modifications in the vesicle (or DNA) double layers when binding occurs.

Acknowledgment. MIUR, the Ministry of University and Scientific Research, is acknowledged for financial support.

References and Notes

(1) Marques, E. F.; Dias, R.; Miguel, M.; Khan, A.; Lindman, B. In *Polymer Gels and Networks*; Osada, Y., Khokhlov, A. R., Eds.; Marcel Dekker: New York, 2002; p 67.
(2) Karukstis, K. K.; McCormack, S. A.; McQueen, T. M.; Goto, K. F. *Langmuir* **2004**, *20*, 64.
(3) Khan, A. *Curr. Opin. Colloid Interface Sci.* **1996**, *1*, 614.
(4) Yuet, P. K.; Blankschtein, D. *Langmuir* **1996**, *12*, 3802.
(5) Dias, R. S.; Lindman, B.; Miguel, M. G. *J. Phys. Chem. B* **2002**, *106*, 12608.
(6) Miguel, M. G.; Pais, A. A. C. P.; Dias, R. S.; Leal, C.; Rosa, M.; Lindman, B. *Colloid Surf., A: Physicochem. Eng. Aspects* **2003**, *228*, 45.
(7) Wheeler, C. J.; Felgner, P. L.; Tsai, Y. J.; Marshall, J.; Sukhu, L.; Doh, S. G.; Hartikka, J.; Nietupski, J.; Manthorpe, M. *Proc. Nat. Acad. Sci. U.S.A.* **1996**, *93*, 11454.
(8) Jung-Hua, S. K.; Ming-Shiou, J.; Chien-Hsiang, C.; Hsuan-Wen, C.; Cih-Ta, L. *Colloids Surf., B: Biointerfaces* **2005**, *41*, 189.
(9) Eliyahu, H.; Servel, N.; Domb, A.; Barenholz, Y. *Gene Ther.* **2002**, *9*, 850.

(10) Simberg, D.; Weisman, S.; Talmon, Y.; Barenholz, Y. *Crit. Rev. Ther. Drug Carrier Syst.* **2004**, *21*, 257.
(11) Muzzalupo, R.; Trombino, S.; Iemma, F.; Puoci, F.; La Mesa, C.; Picci, N. *Colloids Surf., B: Biointerfaces* **2005**, *46*, 78.
(12) De Cuyper, M.; Caluwier, D.; Baert, J.; Cocquyt, J.; Van der Meeren, P. *Z. Phys. Chem. (Muenchen)* **2006**, *220*, 133.
(13) Dias, R. S.; Pais, A. A. C. C.; Miguel, M. G.; Lindman, B. *J. Chem. Phys*. **2003**, *119*, 8150.
(14) Marques, E. F. *Langmuir* **2000**, *16*, 4798.
(15) Grinberg, S.; Linder, C.; Kolot, V.; Waner, T.; Wiesman, Z.; Shaubi, E.; Heldman, E. *Langmuir* **2005**, *21*, 7638.
(16) Gonçalves, E.; Debs, R. J.; Health, T. D. *Biophys. J.* **2004**, *86*, 1554.
(17) Caracciolo, G.; Pozzi, D.; Caminiti, R.; Amenitsch, H. *Chem. Phys. Lett*. **2006**, *429*, 250.
(18) Mel'nikov, S. M.; Mel'nikova, J. S.; Löfroth, J. -E. *J. Phys. Chem. B* **1998**, *102*, 9367.
(19) Moren, A. K.; Regev, O.; Khan, A. *J. Colloid Interface Sci*. **2000**, *222*, 170.
(20) Pevzner, S.; Regev, O.; Lind, A.; Linden, M. *J. Am. Chem. Soc*. **2003**, *125*, 652.
(21) Scarzello, M.; Smisterova, J.; Wagenaar, A.; Stuart, M. C. A.; Hoekstra, D.; Engberts, J. B. F. N.; Hulst, R. *J. Am. Chem. Soc*. **2005**, *127*, 10420.
(22) Yatcilla, M. T.; Herrington, K. L.; Brasher, L. L.; Kaler, E. W.; Chiruvolu, S.; Zasadzinski, J. A. *J. Phys. Chem*. **1996**, *100*, 5874.
(23) Di Ilio, V.; Pasquariello, N.; van der Esch, A. S.; Cristofaro, M.; Scarsella, G.; Risuleo, G. *Mol. Cell. Biochem*. **2006**, *287*, 69.
(24) Bonincontro, A.; Calandrini, V.; Onori, G. *Colloids Surf., B: Biointerfaces* **2001**, *21*, 311.
(25) Athey, T. W.; Stuckly, M. A.; Stuckly, S. S. *IEEE Trans. Microwave Theory Tech.* **1982**, *30*, 82.
(26) Ciurleo, A.; Cinelli, S.; Guidi, M.; Bonincontro, A.; Onori, G.; La Mesa, C. *Biomacromolecules* **2007**, *8*, 399.
(27) Bordi, F.; Cametti, C.; Di Biasio, A.; Angeletti, M.; Sparapani, L. *Bioelectrochemistry* **2000**, *52*, 213.
(28) Provencher, S. W. *Comput. Phys. Commun.* **1982**, *27*, 213.
(29) Gradzielski, M. *J. Phys.: Condens. Matter* **2003**, *15*, R655.
(30) (a) Jung, H. T.; Coldren, B.; Zasadzinski, J. A.; Iampietro, D. J.; Kaler, E. W. *Proc. Natl. Acad. Sci. U.S.A.* **2001**, *98*, 1353. (b) Safran, S. A.; Pincus, P.; Andelman, D. *Science* **1990**, *248*, 354. (c) Safran, S. A.; Pincus, P.; Andelman, MacKintosh, F. C. *Phys. Rev. A: At., Mol., Opt. Phys.* **1991**, *43*, 1071.
(31) Helfrich, W. *Z. Naturforsh., A* **1978**, *33*, 305.
(32) Muzzalupo, R.; Gente, G.; La Mesa, C.; Caponetti, E.; Chillura-Martino, D.; Pedone, L.; Saladino, M. L. *Langmuir* **2006**, *22*, 6001.
(33) Letizia, C.; Andreozzi, P.; Scipioni, A.; Bonincontro, A.; La Mesa, C.; Spigone, E. *J. Phys. Chem. B* **2007**, *111*, 898.
(34) Israelachvili, J. N.; Mitchell, D. J.; Ninham, B. W. *J. Chem. Soc., Faraday Trans. 1* **1976**, *72*, 1525.
(35) Roldan-Toro, R.; Solier, J. D. *J. Colloid Interface Sci*. **2004**, *274*, 76.
(36) Grosse, C. *J. Phys. Chem.* **1988**, *92*, 3905.
(37) Bonincontro, A.; Marchetti, S.; Onori, G. Rosati, A. *Chem. Phys*. **2005**, *312*, 55.
(38) Bonincontro, A.; Spigone, E.; Ruiz Peña, M.; Letizia, C.; La Mesa, C. *J. Colloid Interface Sci.* **2006**, *304*, 342.
(39) Barchini, R.; Pottel, R. *J. Phys. Chem*. **1994**, *98*, 7899.
(40) Bonincontro, A.; Michiotti, P.; La Mesa, C. *J. Phys. Chem. B* **2003**, *107*, 14164.
(41) Bonincontro A.; Cametti C.; Nardiello B.; Marchetti S.; Onori, G. *Biophys. Chem.* **2006**, *20*, 7.
(42) Lee, R. S.; Bone, S. *Biochim. Biophys. Acta: Gene Struct. Expression* **1998**, *1397*, 316.
(43) Tunis-Schneider, M. J. B.; Maestre, M. F. *J. Mol. Biol*. **1970**, *52*, 521.
(44) Rosa, M.; Dias, R.; Miguel, M. daG.; Lindman, B. *Biomacromolecules* **2005**, *6*, 2164.
(45) Costa, D.; Hansson, P.; Schneider, S.; Graca Miguel, M.; Lindman, B. *Biomacromolecules* **2006**, *7*, 1090.

BM0612079